# Bottom Hadrochemistry in High-Energy Hadronic Collisions

Min He[1] and Ralf Rapp[2]
[1]Department of Applied Physics, Nanjing University of Science and Technology, Nanjing 210094, China
[2]Cyclotron Institute and Department of Physics and Astronomy, Texas A&M University, College Station, Texas 77843-3366, USA

(Received 9 October 2022; revised 3 June 2023; accepted 22 June 2023; published 5 July 2023)

The hadrochemistry of bottom quarks ($b$) produced in hadronic collisions encodes valuable information on the mechanism of color neutralization in these reactions. Since the $b$-quark mass is much larger than the typical hadronic scale of ∼1 GeV, $b\bar{b}$ pair production is expected to be well separated from subsequent hadronization processes. A significantly larger fraction of $b$ baryons has been observed in proton-proton ($pp$) and proton-antiproton ($p\bar{p}$) reactions relative to $e^+e^-$ collisions, challenging theoretical descriptions. We address this problem by employing a statistical hadronization approach with an augmented set of $b$-hadron states beyond currently measured ones, guided by the relativistic quark model and lattice-QCD computations. Assuming *relative* chemical equilibrium between different $b$-hadron yields, thermal densities are used as fragmentation weights of $b$ quarks into various hadron species. With quark model estimates of the decay patterns of excited states, the fragmentation fractions of weakly decaying $b$ hadrons are computed and found to agree with measurements in $p\bar{p}$ collisions at the Tevatron. By combining transverse-momentum ($p_T$) distributions of $b$ quarks from perturbative QCD with thermal weights and independent fragmentation toward high $p_T$, a fair description of the $p_T$-dependent $\bar{B}_s^0/B^-$ and $\Lambda_b^0/B^-$ ratios measured in $pp$ collisions at the LHC is obtained. The observed enhancement of $\Lambda_b^0$ production is attributed to the feeddown from thus far unobserved excited $b$ baryons. Finally, we implement the hadrochemistry into a strongly coupled transport approach for $b$ quarks in heavy-ion collisions, utilizing previously determined $b$-quark transport coefficients in the quark-gluon plasma, to highlight the modifications of hadrochemistry and collective behavior of $b$ hadrons in Pb-Pb collisions at the LHC.

DOI: 10.1103/PhysRevLett.131.012301

*Introduction.*—The masses of charm ($c$) and especially bottom ($b$) quarks are much greater than the nonperturbative scale of quantum chromodynamics (QCD), $\Lambda_{\rm QCD}$, and, therefore, their production in experiment offers valuable tests of perturbative-QCD dynamics [1,2]. However, the heavy-quark (HQ) conversion into heavy-flavor (HF) hadrons is an intrinsically soft process that usually requires phenomenological modeling of nonperturbative fragmentation functions (FFs) to describe the production yields and momentum spectra of the observed hadrons [1,3–5]. Fragmentation fractions of heavy quarks into weakly decaying heavy hadrons, which include feeddown from excited states via strong or electromagnetic decays, provide a critical test of hadronization mechanisms and are commonly denoted as $f_u$, $f_d$, $f_s$, and $f_{\rm baryon}$, representing the probabilities of, e.g., a $b$ quark hadronizing into a $B^-$, $\bar{B}^0$, and $\bar{B}_s^0$ meson and a $b$ baryon (or their charge-conjugate counterparts), respectively. Precise knowledge of these fractions is also important to improve the sensitivity of searches for physics beyond the standard model via rare decays of $b$ hadrons [6].

Traditionally, $b$-quark fragmentation has been assumed to be universal across different colliding systems based on the notion that hadronization occurs nonperturbatively at the scale of $\Lambda_{\rm QCD}$ [7] independent of the environment. This is supported, within uncertainties, by measurements of the $f_s/f_d$ ratio that are consistent between $e^+e^-$ collisions at the $Z^0$ resonance at LEP [8,9] and $pp$ collisions at the LHC [10–18]. However, a substantially larger value of $f_{\Lambda_b}/f_d$ has been observed in high-energy $b$ jets produced in $p\bar{p}$ [19] and $pp$ [14,20,21], compared to $b$ jets from $Z^0$ decays [9,22,23], thus challenging the universality assumption. Similar discrepancies have been reported in the charm ($c$) sector [24–26].

In practice, FFs for $b$ or $c$ hadrons are usually inferred from $e^+e^-$ annihilation data. Employing these FFs gives a satisfactory description of $p_T$-differential cross sections for $b$ and $c$ mesons in hadronic collisions within various calculational schemes, such as the fixed order next-to-leading logarithm (FONLL) [27–29], $k_T$ factorization [30–32], or the general-mass variable-flavor number scheme [33–35]. However, the application of FFs for $c$ baryons

substantially underestimates $\Lambda_c$ production, especially at low $p_T$ [32,35], in $pp$ collisions at the LHC [24,25], further questioning their universality. An extraction of the FFs for $b$ baryons is currently lacking [36].

Effects of the partonic environment on HQ hadronization have first been put forward in elementary hadronic collisions [37–43]. Specifically, HQ hadronization may be affected through recombination with valence quarks in the initial state [37–41] or multiparton interactions in the final state [42]. In $pp$ collisions at LHC energies, this has been pursued via a statistical coalescence production of $c$ hadrons [44,45], where hadron yields are determined by the thermostatistical weights governed by their masses at a universal hadronization "temperature" [46–48]. In the present work, we generalize this approach to the bottom sector to compute the $b$ hadrochemistry, using a large set of $b$-hadron states that goes well beyond the currently observed spectrum [49]. By further employing quark model estimates of the decay systematics of excited $b$ hadrons, we are able to predict a large set of fragmentation fractions of weakly decaying $b$ hadrons. We also evaluate the $p_T$ dependence of the hadrochemistry via a combined recombination-fragmentation scheme, which enables predictions for the total $b\bar{b}$ cross section as well as for the $\bar{B}_s^0/B^-$ and $\Lambda_b^0/B^-$ ratios in $pp$ collisions. Finally, we implement the new hadrochemistry into our Langevin transport approach for heavy-ion collisions and highlight predictions for the nuclear modification factor of selected $b$ hadrons in 5 TeV Pb-Pb collisions.

*Bottom-hadron spectrum and strong decays.*—The experimental effort to search for missing resonances in the HF sector has been ongoing for decades [50–52]. The current particle data group (PDG) listings are rather scarce especially for $b$ baryons [49]. Many additional $b$ hadrons are predicted by quark model studies [53–55] and in good agreement with lattice-QCD (lQCD) results [56,57]. We therefore employ a statistical hadronization model (SHM) using two different sets of $b$ hadrons as input: (a) PDG-only states [49] and (b) a relativistic quark model (RQM) [53,54] which additionally includes 18 $B$'s, 16 $B_s$'s, 27 $\Lambda_b$'s, 45 $\Sigma_b$'s, 71 $\Xi_b$'s, and 41 $\Omega_b$'s, up to meson (baryon) masses of 6.5 (7) GeV. Since we are mostly concerned with the *relative* production yields of $b$ hadrons, we use the grand-canonical version of SHM, which works well for bulk hadron production in minimum-bias $pp$ collisions at the LHC energies [58,59] (the smallness of the total number of $b$ hadrons requires a canonical treatment of the $b$ number when computing the *absolute* yields, but the induced canonical suppression factor is common to all $b$ hadron containing a single $b$ quark and, thus, cancels out in hadron ratios [60]; likewise, the $b$ fugacity factor, which is fixed by the total $b\bar{b}$ cross section, is dropped). The thermal density of a given $b$ hadron of mass $m_i$ and spin-isospin degeneracy $d_i$ and containing $N_s^i$ strange or antistrange quarks is then evaluated at the hadronization temperature $T_H$ as

$$n_i^{\text{primary}} = \frac{d_i}{2\pi^2}\gamma_s^{N_s^i} m_i^2 T_H K_2\left(\frac{m_i}{T_H}\right), \tag{1}$$

where $K_2$ is the modified Bessel function of second kind and $\gamma_s \sim 0.6$ [45,61] the strangeness suppression factor in elementary reactions. While the SHM analysis of light-hadron yields in heavy-ion collisions at the LHC [48] indicates a hadronization temperature very comparable to the pseudocritical chiral transition temperature $T_{\text{pc}}^{\chi} \sim 155$ MeV determined in lQCD [62,63], a higher hadronization temperature $T_H \sim 170$ MeV appears to be more appropriate for HF hadrons in elementary reactions [44]. A flavor hierarchy in the effective hadronization temperature has also been suggested based on lattice calculations of quark flavor susceptibilities [64]. In the following, we therefore use $T_H = 170$ MeV as the default value and $T_H = 160$ MeV as part of our error estimate.

Information about decays of excited $b$ hadrons into their weakly decaying ground states is very limited, even for observed states [49]. Instead of taking rather incomplete results available in the literature, we estimate the branching ratios (BRs) of the OZI-allowed strong decays for all employed $b$ hadrons within the $^3P_0$ pair creation model [65]. As schematically shown in Fig. 1, a pair of quarks with $J^{PC} = 0^{++}$ is created from the vacuum and regroups with the quarks within the initial $b$ hadron into the outgoing meson or baryon. For example, in the case of a baryon decay, there are three ways of quark regrouping [66], leading to a $b$ baryon plus a light meson or a $b$ meson plus a light baryon in the final state; cf. Fig. 1(b). We do not attempt to perform full calculations using realistic hadron wave functions [67–69] but obtain the needed BRs via counting all possible diagrams of the types in Fig. 1 once a decay channel opens up, by assuming the number of diagrams for the channel to be proportional to its BR. The probability of creating a quark pair is assumed to be $\propto e^{-2m_q/T_H}$; therefore, a diagram involving creating a $s\bar{s}$ is weighted by $e^{-2m_s/T_H}/e^{-2m_{u/d}/T_H} \simeq 1/3$ taking the current-quark masses $m_{u/d} \simeq 8$ MeV and $m_s \simeq 100$ MeV (this estimate is robust even if constituent-quark masses are

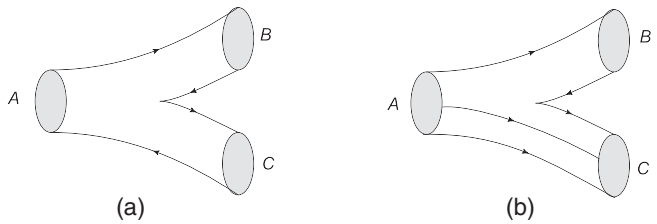


FIG. 1. The (a) meson and (b) baryon decay process $A \to B + C$ in the $^3P_0$ model.

used). We account for direct three-body decays of $b$ baryons by counting the regroupings resulting from creation of two $u\bar{u}$ or $d\bar{d}$ pairs and find significant BRs for the $\Lambda_b^0 + n\pi$ channels of the excited $\Lambda_b$'s or $\Sigma_b$'s decays, which is supported by the measured information on $\Lambda_b(5912)^0$ and $\Lambda_b(5920)^0$ [reminiscent of $\Lambda_c(2595)^+$ and $\Lambda_c(2625)^+$ in the $c$ sector] [49]. While low-lying excited states all end up in their corresponding ground states (including the pure electromagnetic decay of $B^*$ and $B_s^*$), higher states have significant cross-feeddowns, e.g., BR $\sim 14\%$ for excited $B$'s to $\bar{B}_s^0 + K$, ~85%–100% for excited $B_s$'s to $B^-/\bar{B}^0 + K$, ~20%–30% for excited $\Lambda_b$'s ($\Sigma_b$'s) to $B^-(\bar{B}^0) + N$, ~20% (20%) for excited $\Xi_b$'s to $\Lambda_b^0 + \pi + K$ ($B^-/\bar{B}^0 + \Sigma$), and ~75% (~25%) for excited $\Omega_b$'s to $\Xi_b^{0-} + K$ ($B^-/\bar{B}^0 + \Xi$). These estimates are overall consistent with available results from a relativized quark model [68,69].

*Bottom-hadron fractions and ratios.*—With the BRs as estimated above, the total densities of the weakly decaying ground states are obtained via

$$n_\alpha = n_\alpha^{\text{primary}} + \sum_i n_i^{\text{primary}} \cdot \text{BR}(i \to \alpha). \tag{2}$$

These densities are converted into fractions of the total $b$ content in Table I, under the constraint of $f_u + f_d + f_s + f_{\Lambda_b^0} + f_{\Xi_b^{0,-}} + f_{\Omega_b^-} = 1$ when neglecting the tiny fractions of states made of two or more heavy quarks (e.g., $B_c$ mesons, doubly bottom baryons, or bottomonia). When going from the PDG to the RQM scenario, a marked transfer of the $b$ content from the meson to the baryon sector occurs, comparable to the experimentally observed $b$-hadron fractions in $e^+e^-$ vs $p\bar{p}$ collisions [23] (and reminiscent of the charm sector [26]). Specifically, the fraction of $B^-$ ($\bar{B}_s^0$) is reduced by ~10% (15%), but the fractions of $\Lambda_b^0$ and $\Xi_b^{0,-}$ are both enhanced by ~50% upon inclusion of additional baryons in the RQM at $T_H = 170$ MeV, relative to the PDG scenario (similarly at $T_H = 160$ MeV). The weakly decaying $b$-hadron fractions obtained in the RQM for both $T_H = 170$ and 160 MeV turn out to agree with the measurements in $p\bar{p}$ collisions at the Tevatron within uncertainties: $f_u = f_d = 0.340 \pm 0.021$, $f_s = 0.101 \pm 0.015$, and $f_{\text{baryon}} = 0.220 \pm 0.048$ [23].

TABLE I. Fractions of ground-state $b$ hadrons (relative to total $b\bar{b}$) from the SHM with $T_H = 170$ and 160 MeV in the PDG and RQM scenarios. $\Xi_b^{0,-}$ denotes the sum of two isospin states. The $\Omega_b^-$ fraction is ~0.1% (not shown here).

| $f_\alpha$ | $B^-$ | $\bar{B}^0$ | $\bar{B}_s^0$ | $\Lambda_b^0$ | $\Xi_b^{0,-}$ |
|---|---|---|---|---|---|
| PDG(170) | 0.3697 | 0.3695 | 0.1073 | 0.1157 | 0.036 98 |
| PDG(160) | 0.3782 | 0.3780 | 0.1094 | 0.1023 | 0.031 44 |
| RQM(170) | 0.3391 | 0.3389 | 0.091 52 | 0.1737 | 0.055 03 |
| RQM(160) | 0.3533 | 0.3532 | 0.096 20 | 0.1502 | 0.045 65 |

The calculated ratios of $\bar{B}^0$, $\bar{B}_s^0$, $\Lambda_b^0$, and $\Xi_b^{0,-}$ to $B^-$ are summarized in Table II. The mesonic ratios are rather stable, but baryonic ratios are more sensitive to variations in the hadronization temperature. While an equal production of $B^-$ and $\bar{B}^0$ always holds due to isospin symmetry, the $\bar{B}_s^0/B^-$ ratio is reduced by ~7% upon inclusion of additional states in the RQM scenario. The most pronounced effect is caused by the inclusion of missing baryons, enhancing the baryonic ratios by ~60% relative to the PDG scenario, leading to $\Lambda_b^0/B^- \sim 0.51$ with $T_H = 170$ MeV, rather comparable to $f_{\Lambda_b^0}/(f_u + f_d) = 0.259 \pm 0.018$ as measured by LHCb in 13 TeV $pp$ collisions [14].

*Bottom-hadron $p_T$ spectra in $pp$ collisions.*—To compute the $p_T$ differential cross sections of ground-state $b$ hadrons, we simulate the fragmentation and decay processes using the $b$-quark $p_t$ spectrum in $\sqrt{s} = 5.02$, 7, and 13 TeV $pp$ collisions from FONLL [27,28]. A $b$ quark sampled from the spectrum is fragmented into $b$ hadrons via the same FF [3] as implemented in FONLL:

$$D_{b\to H_b}(z) \propto z^\alpha (1-z), \tag{3}$$

where $z = p_T/p_t$ is the fraction of the $b$ hadron's ($H_b$) momentum, $p_T$, over the $b$-quark momentum, $p_t$. The fragmentation weight of $H_b$ is determined by its thermal density $n_{H_b}^{\text{primary}}$ [Eq. (1)], normalized by the sum $\sum_{H_b} n_{H_b}^{\text{primary}}$. Each $H_b$ produced from fragmentation is then decayed into the ground-state particles with a constant matrix element, i.e., decay kinematics solely determined by phase space and BRs estimated above.

The parameter $\alpha$ in Eq. (3) is tuned to fit the slope of the $p_T$ spectra of ground-state $b$ hadrons (kinematic effects from recombination are partially absorbed by this tune). For the RQM scenario at $T_H = 170$ MeV, we find that with $\alpha_B = 45$ (for simplicity taken the same for all $B$ mesons; similarly, $\alpha_{B_s} = 25$ for all $B_s$ mesons and $\alpha_{\text{baryon}} = 8$ for all $b$ baryons), the measured $B^+ + B^-$ $p_T$-differential cross section at $2 < y < 2.5$ [70] can be described with a total $b\bar{b}$ cross section of $d\sigma^{b\bar{b}}/dy = 34.55$ μb (68.87 μb) in $\sqrt{s} =$ 7 TeV (13 TeV) $pp$ collisions; cf. Fig. 2(a). The latter is a prediction based on the computed hadrochemistry content and is consistent with the LHCb data for semileptonic $b$ decays [71]. For the PDG scenario, the $B^+ + B^-$ data turn out to be equally well described but with an ~10% smaller

TABLE II. Ratios of $\bar{B}^0$, $\bar{B}_s^0$, $\Lambda_b^0$, and $\Xi_b^{0,-}$ to $B^-$ at $T_H = 170$ and 160 MeV in the PDG and RQM scenarios.

| $r_\alpha$ | $\bar{B}^0/B^-$ | $\bar{B}_s^0/B^-$ | $\Lambda_b^0/B^-$ | $\Xi_b^{0,-}/B^-$ |
|---|---|---|---|---|
| PDG(170) | 0.9995 | 0.2904 | 0.3129 | 0.1000 |
| PDG(160) | 0.9995 | 0.2894 | 0.2706 | 0.083 13 |
| RQM(170) | 0.9994 | 0.2699 | 0.5122 | 0.1623 |
| RQM(160) | 0.9996 | 0.2723 | 0.4250 | 0.1292 |

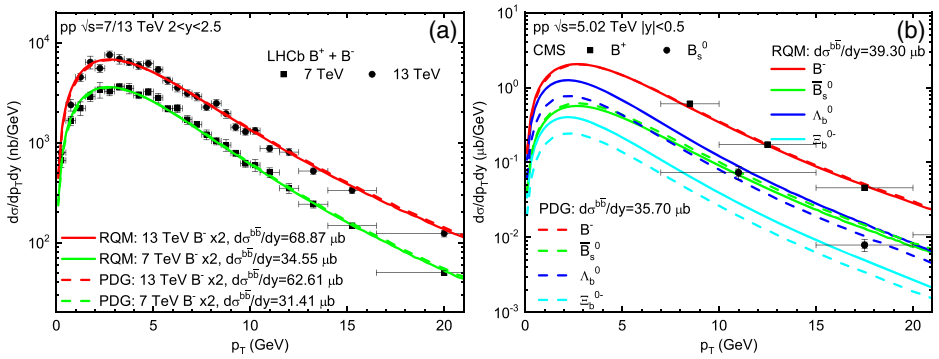


FIG. 2. (a) $p_T$-differential cross sections of ground-state $B^-$ in $\sqrt{s} = 7$ and 13 TeV $pp$ collisions for the RQM (solid lines) and PDG (dashed lines) scenarios at $T_H = 170$ MeV, in comparison with LHCb data at $2 < y < 2.5$ [70]. (b) The same for $B^-$, $\bar{B}_s^0$, $\Lambda_b^0$, and $\Xi_b^{0,-}$ in $\sqrt{s} = 5.02$ TeV $pp$ collisions at midrapidity, compared to $|y| < 2.4$ CMS data [72,73] scaled to $|y| < 0.5$ via FONLL [27,28].

total $b\bar{b}$ cross section. The decrease in the latter is due to the reduction of $b$ content in the baryon sector, as demonstrated by the significantly smaller $p_T$-differential yields of $\Lambda_b^0$ and $\Xi_b^{0,-}$ compared to their RQM counterparts; cf. Fig. 2(b) for $\sqrt{s} = 5.02$ TeV $pp$ collisions at midrapidity, where available data for $B^+$ and $B_s^0$ are compared; the value $d\sigma^{b\bar{b}}/dy = 39.30$ μb deduced from the RQM scenario is comparable to the value measured by ALICE via nonprompt $D$ mesons [17].

We now turn to the $p_T$-dependent $b$-hadron ratios. For $\bar{B}_s^0/B^-$, shown in Fig. 3(a), the additional states in the RQM scenario reduce the PDG scenario results by over 10% at low $p_T$, improving the description of the LHCb data for $f_s/f_d$ which are approximately constant with $p_T$. For $\Lambda_b^0/B^-$, the RQM scenario is clearly favored by the LHCb data; cf. Fig. 3(b). The substantial gap between data and the PDG scenario results is largely overcome by the feeddown of the large set of "missing" baryons included in the RQM calculation, leading to a fair description of the data, including its increasing trend toward low $p_T$. For comparison, the LEP average of $f_{\Lambda_b}/f_d$ [23] in $Z$ decays is indicated as a horizontal arrow. Finally, our predictions for the $\Xi_b^{0,-}/B^-$ ratio from RQM and PDG scenarios are compared in Fig. 3(c), exhibiting similar features as in the case of $\Lambda_b^0/B^-$.

*Bottom hadrons in PbPb collisions.*—The hadrochemistry computed above in $pp$ collisions serves as a controlled reference for studying modifications in heavy-ion collisions. Toward this end, we employ a strongly coupled transport approach previously developed for the $c$ sector [43] and calculate the hadrochemistry and nuclear modification factor of $b$ hadrons in $\sqrt{s_{NN}} = 5.02$ TeV PbPb collisions. In this approach, the $b$-quark diffusion in the hydrodynamically evolving quark-gluon plasma (QGP) is simulated via relativistic Langevin equations whose accuracy is improved compared to $c$ quarks because of the ∼3 times larger $b$-quark mass (no shadowing is put on the initial $b$-quark spectrum). The transport coefficient is taken from lQCD-potential-based $T$-matrix computations [75] but amplified by the same $K = 1.6$ factor as done for the $c$ sector [43], to mimic missing contributions from spin-dependent forces [76] and/or radiative energy loss.

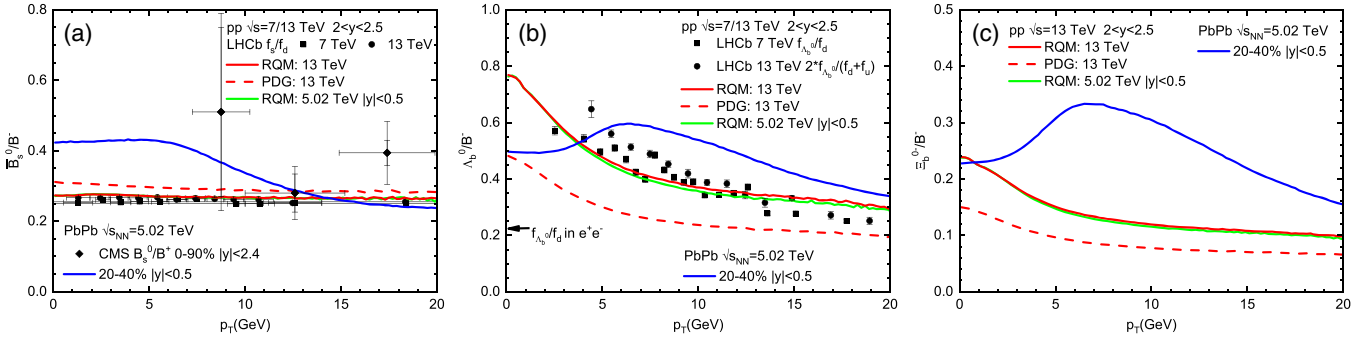


FIG. 3. $p_T$-dependent ratios of (a) $\bar{B}_s^0/B^-$, (b) $\Lambda_b^0/B^-$, and (c) $\Xi_b^{0,-}/B^-$ for RQM (solid lines) and PDG (dashed lines) scenarios in $\sqrt{s} = 13$ (red, $2 < y < 2.5$) and 5.02 TeV (green, $|y| < 0.5$) $pp$ collisions, together with ratios in $\sqrt{s_{NN}} = 5.02$ TeV PbPb collisions (blue solid lines, 20%–40% centrality) at midrapidity, in comparison with available LHCb [14,15,20] and CMS [74] data. The horizontal arrow in the middle panel indicates the LEP average for $f_{\Lambda_b}/f_d$ [23] from $Z^0$ decays at an average $b$-quark transverse momentum of $\langle p_t(b) \rangle \sim 40$ GeV.

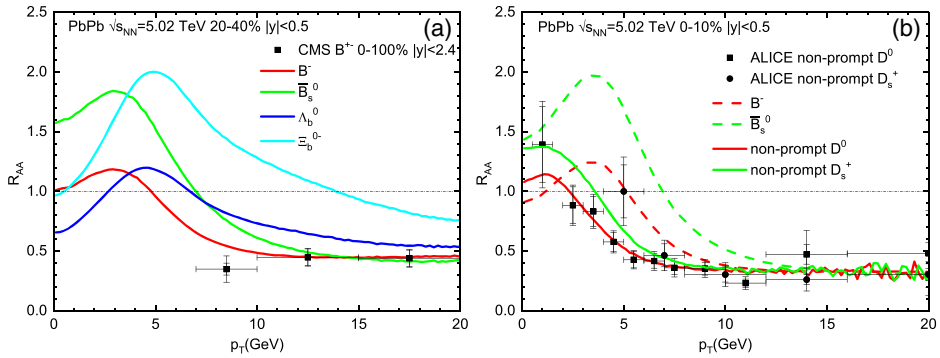


FIG. 4. (a) Nuclear modification factors for ground-state $B^-$, $\bar{B}_s^0$, $\Lambda_b^0$, and $\Xi_b^{0,-}$ in 20%–40% $\sqrt{s_{NN}} = 5.02$ TeV PbPb collisions at midrapidity, together with CMS data for $B^{+-}$ in 0%–100% centrality [72]. (b) The same for nonprompt $D^0$ and $D_s^+$ (0%–10% centrality) in comparison with ALICE data [83,84].

At $T_H = 170$ MeV, $b$-quark hadronization into mesons or baryons is computed by the 4-momentum-conserving resonance recombination model (RRM) [43,77]. The RRM is implemented event by event in combination with the Langevin diffusion based on self-consistently determined recombination probabilities $P_i(p_b^*)$ [43]. The sum of $\sum_i P_i(p_b^*)$ over all primary $b$ hadrons $i$ is renormalized to unity at vanishing $b$-quark rest-frame momentum ($p_b^*$) to guarantee the majority of low-momentum $b$ quarks hadronize through recombination, while leftover $b$ quarks, as a result of the decreasing $\sum_i P_i(p_b^*)$ toward large $p_b^*$, fragment in the same manner as in $pp$. A prominent feature of our RRM implementation is the inclusion of space-momentum correlations (SMCs) in the quark phase-space distributions [43], which augments the flow effect in the $p_T$ spectra of high-mass $b$ hadrons and generally extends the reach of recombination toward higher $p_T$.

In practice, constituent-quark ($m_{u,d} = 0.33$ GeV, $m_s = 0.45$ GeV, $m_b = 4.88$ GeV) and -diquark masses (scalar $m_{[ud]} = 0.71$ GeV within $\Lambda_b$'s, axial-vector $m_{\{ud\}} = 0.909$ GeV within $\Sigma_b$'s, $m_{[us]} = 0.948$ GeV and $m_{\{us\}} = 1.069$ GeV within $\Xi_b$'s, and $m_{\{ss\}} = 1.203$ GeV within $\Omega_b$'s) are taken from RQM studies [53,54]. We use energy-dependent widths (cf. Ref. [78]) with on-shell values of $\Gamma^0 \sim 0.1$ GeV in the meson, diquark, and baryon cross sections in RRM, which suppresses artificial low-$s$ tails of the pertinent Breit-Wigner amplitudes for $\sqrt{s}$ values far below the nominal resonance mass (thereby significantly reducing the sensitivity of final results to variations of the width values).

Primary $b$ hadrons formed from hadronization undergo further diffusion in the hadronic phase until kinetic freeze-out using our previously calculated $D$-meson thermalization rate [79] scaled down by the $b$-hadron mass. These hadrons are then decayed to obtain the $p_T$ spectra of ground-state $b$ hadrons. The ratios of $\bar{B}_s^0/B^-$, $\Lambda_b^0/B^-$, and $\Xi_b^{0,-}/B^-$ are shown in Fig. 3. Compared to their counterparts in $pp$ collisions, the $\bar{B}_s^0/B^-$ ratio exhibits a significant enhancement up to $p_T \sim 10$ GeV, resulting from $b$-quark coupling to the enhanced strangeness in QGP through recombination; an enhanced $\Lambda_b^0/B^-$ ratio appears in the intermediate-$p_T$ region due to a stronger flow effect on generally heavier baryons as captured by RRM with SMCs, peaking at a higher $p_T \sim 6$ GeV and extending to significantly larger $p_T \sim 15$ GeV than the corresponding ratio in the $c$ sector [43,80] because of the larger $b$-quark mass. The $\Xi_b^{0,-}/B^-$ ratio develops a more pronounced enhancement, as it combines the strange-quark and baryon features. The nuclear modification factors $R_{AA}$, defined as the ratio of $p_T$ differential yield in PbPb collisions to the cross section in $pp$ collisions scaled by the nuclear overlap function [81], are shown in Fig. 4(a) for ground-state $B^-$ (same for $\bar{B}^0$), $\bar{B}_s^0$, $\Lambda_b^0$, and $\Xi_b^{0,-}$ in semicentral PbPb collisions, with an expected hierarchy of flow effects and suppression driven by their quark content. Upon weak decay of these hadrons into nonprompt $c$ hadrons utilizing PYTHIA8 [82], the resulting $R_{AA}$'s for nonprompt $D^0$ and $D_s^+$ in central collisions show fair agreement with ALICE data; cf. Fig. 4(b).

*Summary.*—Employing the statistical hadronization model, we have evaluated the hadrochemistry of $b$ hadrons in $pp$ collisions at collider energies. The spectrum of $b$ hadrons has been taken from theoretical predictions of the relativistic quark model which is largely supported by lattice-QCD computations of vacuum spectroscopy. Many of the RQM states, especially in the baryon sector, are not yet observed and are, therefore, much more numerous than the current PDG listings. With strong and electromagnetic feeddown estimated from the $^3P_0$ model, we have performed quark model estimates of excited $b$-hadron decays which enabled a comprehensive prediction of fragmentation fractions of weakly decaying $b$ hadrons for the first time; pertinent ratios turn out to agree with measurements in $p\bar{p}$ collisions at the Tevatron. We have further calculated $p_T$ differential cross sections for ground-state $b$ hadrons using fragmentation weights of an underlying (perturbative) $b$-quark spectrum determined by the SHM.

The resulting $p_T$-dependent $\bar{B}_s^0/B^-$ and $\Lambda_b^0/B^-$ ratios agree with LHCb data. All of our results critically depend on the excited states that the RQM predicts beyond the PDG listings. We have furthermore deployed the new hadrochemistry into our strongly coupled HF transport model for heavy-ion collisions, to evaluate spectral modifications in PbPb collisions. The $p_T$-dependent modifications of ratios between different ground-state $b$ hadrons have been quantified, highlighting the role of $b$ quarks as probes of the QGP—a central pillar of experimental efforts at both RHIC [85] and the LHC in the near future [86–89].

This work was supported by National Natural Science Foundation of China (NSFC) Grant No. 12075122 and the U.S. National Science Foundation under Grant No. PHY-1913286. M. H. thanks Fabrizio Grosa for help with the simulation of weak decays of $b$ hadrons.

[1] E. Norrbin and T. Sjostrand, Eur. Phys. J. C **17**, 137 (2000).
[2] M. L. Mangano, P. Nason, and G. Ridolfi, Nucl. Phys. **B373**, 295 (1992).
[3] V. G. Kartvelishvili, A. K. Likhoded, and V. A. Petrov, Phys. Lett. **78B**, 615 (1978).
[4] C. Peterson, D. Schlatter, I. Schmitt, and P. M. Zerwas, Phys. Rev. D **27**, 105 (1983).
[5] E. Braaten, K. m. Cheung, S. Fleming, and T. C. Yuan, Phys. Rev. D **51**, 4819 (1995).
[6] V. Khachatryan *et al.* (CMS and LHCb Collaborations), Nature (London) **522**, 68 (2015).
[7] M. Lisovyi, A. Verbytskyi, and O. Zenaiev, Eur. Phys. J. C **76**, 397 (2016).
[8] D. Buskulic *et al.* (ALEPH Collaboration), Phys. Lett. B **361**, 221 (1995).
[9] J. Abdallah *et al.* (DELPHI Collaboration), Phys. Lett. B **576**, 29 (2003).
[10] R. Aaij *et al.* (LHCb Collaboration), Phys. Rev. Lett. **107**, 211801 (2011).
[11] R. Aaij *et al.* (LHCb Collaboration), Phys. Rev. D **85**, 032008 (2012).
[12] R. Aaij *et al.* (LHCb Collaboration), J. High Energy Phys. 04 (2013) 001.
[13] G. Aad *et al.* (ATLAS Collaboration), Phys. Rev. Lett. **115**, 262001 (2015).
[14] R. Aaij *et al.* (LHCb Collaboration), Phys. Rev. D **100**, 031102 (2019).
[15] R. Aaij *et al.* (LHCb Collaboration), Phys. Rev. Lett. **124**, 122002 (2020).
[16] R. Aaij *et al.* (LHCb Collaboration), Phys. Rev. D **104**, 032005 (2021).
[17] S. Acharya *et al.* (ALICE Collaboration), J. High Energy Phys. 05 (2021) 220.
[18] CMS Collaboration, arXiv:2212.02309.
[19] T. Aaltonen *et al.* (CDF Collaboration), Phys. Rev. D **77**, 072003 (2008).
[20] R. Aaij *et al.* (LHCb Collaboration), J. High Energy Phys. 08 (2014) 143.
[21] R. Aaij *et al.* (LHCb Collaboration), Chin. Phys. C **40**, 011001 (2016).
[22] R. Barate *et al.* (ALEPH Collaboration), Eur. Phys. J. C **5**, 205 (1998).
[23] Y. S. Amhis *et al.* (HFLAV Collaboration), Eur. Phys. J. C **81**, 226 (2021).
[24] S. Acharya *et al.* (ALICE Collaboration), J. High Energy Phys. 04 (2018) 108.
[25] S. Acharya *et al.* (ALICE Collaboration), Phys. Rev. Lett. **127**, 202301 (2021).
[26] S. Acharya *et al.* (ALICE Collaboration), Phys. Rev. D **105**, L011103 (2022).
[27] S. Frixione, P. Nason, and G. Ridolfi, J. High Energy Phys. 09 (2007) 126.
[28] M. Cacciari, S. Frixione, N. Houdeau, M. L. Mangano, P. Nason, and G. Ridolfi, J. High Energy Phys. 10 (2012) 137.
[29] S. Catani, S. Devoto, M. Grazzini, S. Kallweit, and J. Mazzitelli, J. High Energy Phys. 03 (2021) 029.
[30] S. Catani, M. Ciafaloni, and F. Hautmann, Nucl. Phys. **B366**, 135 (1991).
[31] J. C. Collins and R. K. Ellis, Nucl. Phys. **B360**, 3 (1991).
[32] R. Maciuła and A. Szczurek, Phys. Rev. D **98**, 014016 (2018).
[33] B. A. Kniehl, G. Kramer, I. Schienbein, and H. Spiesberger, Eur. Phys. J. C **41**, 199 (2005).
[34] B. A. Kniehl, G. Kramer, I. Schienbein, and H. Spiesberger, Phys. Rev. D **84**, 094026 (2011).
[35] B. A. Kniehl, G. Kramer, I. Schienbein, and H. Spiesberger, Phys. Rev. D **101**, 114021 (2020).
[36] G. Kramer and H. Spiesberger, Chin. Phys. C **42**, 083102 (2018).
[37] R. C. Hwa, Phys. Rev. D **51**, 85 (1995).
[38] E. Cuautle, G. Herrera, and J. Magnin, Eur. Phys. J. C **2**, 473 (1998).
[39] E. Braaten, Y. Jia, and T. Mehen, Phys. Rev. Lett. **89**, 122002 (2002).
[40] R. Rapp and E. V. Shuryak, Phys. Rev. D **67**, 074036 (2003).
[41] A. V. Berezhnoy and A. K. Likhoded, Phys. At. Nucl. **78**, 292 (2015).
[42] J. R. Christiansen and P. Z. Skands, J. High Energy Phys. 08 (2015) 003.
[43] M. He and R. Rapp, Phys. Rev. Lett. **124**, 042301 (2020).
[44] A. Andronic, F. Beutler, P. Braun-Munzinger, K. Redlich, and J. Stachel, Phys. Lett. B **678**, 350 (2009).
[45] M. He and R. Rapp, Phys. Lett. B **795**, 117 (2019).
[46] P. Braun-Munzinger, K. Redlich, and J. Stachel, Particle production in heavy ion collisions, in *Quark-Gluon Plasma 3* (World Scientific, Singapore, 2004).
[47] F. Becattini, arXiv:0901.3643.
[48] A. Andronic, P. Braun-Munzinger, K. Redlich, and J. Stachel, Nature (London) **561**, 321 (2018).
[49] P. A. Zyla *et al.* (Particle Data Group), Prog. Theor. Exp. Phys. **2020**, 083C01 (2020).
[50] V. Crede and W. Roberts, Rep. Prog. Phys. **76**, 076301 (2013).
[51] H. X. Chen, W. Chen, X. Liu, Y. R. Liu, and S. L. Zhu, Rep. Prog. Phys. **80**, 076201 (2017).
[52] M. Charles, https://tel.archives-ouvertes.fr/tel-01340092.
[53] D. Ebert, R. N. Faustov, and V. O. Galkin, Eur. Phys. J. C **66**, 197 (2010).

[54] D. Ebert, R. N. Faustov, and V. O. Galkin, Phys. Rev. D **84**, 014025 (2011).
[55] W. Roberts and M. Pervin, Int. J. Mod. Phys. A **23**, 2817 (2008).
[56] R. Lewis and R. M. Woloshyn, Phys. Rev. D **79**, 014502 (2009).
[57] Z. S. Brown, W. Detmold, S. Meinel, and K. Orginos, Phys. Rev. D **90**, 094507 (2014).
[58] N. Sharma, J. Cleymans, B. Hippolyte, and M. Paradza, Phys. Rev. C **99**, 044914 (2019).
[59] S. Das, D. Mishra, S. Chatterjee, and B. Mohanty, Phys. Rev. C **95**, 014912 (2017).
[60] Y. Chen and M. He, Phys. Lett. B **815**, 136144 (2021).
[61] B. I. Abelev *et al.* (STAR Collaboration), Phys. Rev. C **79**, 034909 (2009).
[62] A. Bazavov, T. Bhattacharya, C. DeTar, H. T. Ding, S. Gottlieb *et al.* (HotQCD Collaboration), Phys. Rev. D **90**, 094503 (2014).
[63] S. Borsanyi, Z. Fodor, C. Hoelbling, S. D. Katz, S. Krieg, and K. K. Szabo, Phys. Lett. B **730**, 99 (2014).
[64] R. Bellwied, S. Borsanyi, Z. Fodor, S. D. Katz, and C. Ratti, Phys. Rev. Lett. **111**, 202302 (2013).
[65] S. Capstick and W. Roberts, Prog. Part. Nucl. Phys. **45**, S241 (2000).
[66] C. Chen, X. L. Chen, X. Liu, W. Z. Deng, and S. L. Zhu, Phys. Rev. D **75**, 094017 (2007).
[67] W. Roberts and B. Silvestre-Brac, Few-Body Syst. **11**, 171 (1992).
[68] J. Ferretti and E. Santopinto, Phys. Rev. D **97**, 114020 (2018).
[69] G. L. Yu, Z. Y. Li, Z. G. Wang, J. Lu, and M. Yan, Nucl. Phys. **B990**, 116183 (2023).
[70] R. Aaij *et al.* (LHCb Collaboration), J. High Energy Phys. 12 (2017) 026.
[71] R. Aaij *et al.* (LHCb Collaboration), Phys. Rev. Lett. **118**, 052002 (2017); **119**, 169901(E) (2017).
[72] A. M. Sirunyan *et al.* (CMS Collaboration), Phys. Rev. Lett. **119**, 152301 (2017).
[73] A. M. Sirunyan *et al.* (CMS Collaboration), Phys. Lett. B **796**, 168 (2019).
[74] A. Tumasyan *et al.* (CMS Collaboration), Phys. Lett. B **829**, 137062 (2022).
[75] F. Riek and R. Rapp, Phys. Rev. C **82**, 035201 (2010).
[76] Z. Tang and R. Rapp, arXiv:2304.02060.
[77] L. Ravagli and R. Rapp, Phys. Lett. B **655**, 126 (2007).
[78] V. Vovchenko, M. I. Gorenstein, and H. Stoecker, Phys. Rev. C **98**, 034906 (2018).
[79] M. He, R. J. Fries, and R. Rapp, Phys. Lett. B **701**, 445 (2011).
[80] S. Acharya *et al.* (ALICE Collaboration), Phys. Lett. B **839**, 137796 (2023).
[81] ALICE Collaboration, Centrality determination in heavy ion collisions, Report No. ALICE-PUBLIC-2018-011.
[82] T. Sjöstrand, S. Ask, J. R. Christiansen, R. Corke, N. Desai, P. Ilten, S. Mrenna, S. Prestel, C. O. Rasmussen, and P. Z. Skands, Comput. Phys. Commun. **191**, 159 (2015).
[83] S. Acharya *et al.* (ALICE Collaboration), J. High Energy Phys. 12 (2022) 126.
[84] ALICE Collaboration, arXiv:2204.10386.
[85] C. Dean (Sphenix Collaboration), Proc. Sci. ICHEP2020 (**2021**) 731.
[86] Z. Citron, A. Dainese, J. F. Grosse-Oetringhaus, J. M. Jowett, Y. J. Lee, U. A. Wiedemann, M. Winn, A. Andronic, F. Bellini, E. Bruna *et al.*, CERN Yellow Rep. Monogr. **7**, 1159 (2019).
[87] Letter of intent for ALICE 3: A next generation heavy-ion experiment at the LHC, https://cds.cern.ch/record/2803563?ln=en (2022).
[88] LHCb Collaboration, Future physics potential of LHCb, Report No. LHCb-PUB-2022-012.
[89] ALICE Collaboration, arXiv:2211.04384.